Chemical Science

EDGE ARTICLE

View Article Online
View Journal | View Issue

Cite this: *Chem. Sci.*, 2015, **6**, 4650

Regioselective thioacetylation of chitosan end-groups for nanoparticle gene delivery systems†

V. D. Pickenhahn,[a] V. Darras,[a] F. Dziopa,[a] K. Biniecki,[b] G. De Crescenzo,[a] M. Lavertu*[a] and M. D. Buschmann*[a]

Received 6th January 2015
Accepted 6th May 2015

DOI: 10.1039/c5sc00038f

www.rsc.org/chemicalscience

Chitosan (CS) end-group chemistry is a conjugation strategy that has been minimally exploited in the literature to date. Although the open-chain form of the CS reducing extremity bears a reactive aldehyde moiety, the most common method to generate a reactive end-group on CS is nitrous acid depolymerization, which produces a 2,5-anhydro-D-mannose unit (M-Unit) bearing also an aldehyde moiety. However, the availability of the latter might be low, since previous literature suggests that its hydrated and non-reactive form, namely the *gem*-diol form, is predominant in acidic aqueous conditions. Oxime-click chemistry has been used to react on such aldehydes with various degrees of success, but the use of a co-solvent and additional chemical reagents remain necessary to obtain the desired and stable covalent linkage. In this study, we have assessed the availability of the aldehyde reactive form on chitosan treated with nitrous acid. We have also assessed its reactivity towards thiol-bearing molecules in acidic conditions where CS amino groups are fully protonated and thus unreactive towards aldehyde. LC-MS and NMR spectroscopy methods (^{1}H and DOSY, respectively) confirmed the regioselective thioacetylation of the reactive aldehyde with conversion rates between 55 and 70% depending on the thiol molecule engaged. The stabilization of the hemithioacetal intermediates into the corresponding thioacetals was also found to be facilitated upon freeze-drying of the reaction medium. The PEGylation of the CS M-Unit aldehyde by thioacetylation was also performed as a direct application of the proposed conjugation approach. CS-*b*-PEG$_2$ block copolymers were successfully synthesized and were used to prepare block ionomer complexes with plasmid DNA, as revealed by their spherical morphology *vs.* the rod-like/globular/toroidal morphology observed for polyplexes prepared using native unmodified chitosan. This novel aqueous thiol-based conjugation strategy constitutes an alternative to the oxime-click pathway; it could be applicable to other polymers.

Introduction

Chitosan (CS), a linear and cationic polysaccharide composed of D-glucosamine ($GlcNH_2$) and *N*-acetyl-D-glucosamine (GlcNHAc) units, is derived from chitin by deacetylation. This non-toxic polyelectrolyte holds great interest due to its biocompatibility, biodegradability and mucoadhesive properties.[1] Chitosan and its derivatives have been proposed for applications including gene and drug delivery, tissue repair, water purification and cosmetics.[2–6] Two general approaches have been explored to chemically modify CS: lateral "graft" and "block" modifications. The former involves conjugation to CS lateral functional groups (amine or hydroxyl) whereas the latter relies on conjugation to CS end-groups.

Several strategies for grafting onto CS amines (*N*-2-graft) have been proposed in the literature. For example, PEG and other graft-copolymers have been proposed to enhance CS solubility at physiological pH and increase the colloidal stability of CS-based polyelectrolyte complexes,[7,8] while ligands for specific cell targeting[9,10] or fluorescent dyes[11,12] have also been grafted onto CS amines. However, lateral grafting can potentially compromise the ability of CS to bind nucleic acid and thus limit the stability and efficiency of chitosan/nucleic acid polyelectrolyte complexes for gene delivery applications. Indeed, lateral grafting can impede the ability of CS to electrostatically bind to negatively charged species by reducing its effective charge density and by potentially creating steric hindrance with bulky moieties.[4] Alternatively, the O-6 grafting approach has been proposed to overcome the charge density reduction issue, although grafting of a bulky moiety at this position is likely to create steric hindrance and hence limit complexation with oppositely charged polymers or molecules as well. Additionally, O-6 grafting is technically challenging as it necessitates protection–deprotection steps for the CS amine moieties.[13]

[a]*Dept. Chemical Engineering and Inst. Biomedical Engineering, Ecole Polytechnique, Montreal, QC, Canada. E-mail: marc.lavertu@polymtl.ca; michael.buschmann@polymtl.ca*

[b]*ANRis Pharmaceuticals Inc., Kirkland, QC, Canada*

† Electronic supplementary information (ESI) available. See DOI: 10.1039/c5sc00038f

To overcome these limitations, CS block conjugation strategies (*e.g.*, branched CS,[14,15] PEGylation,[16] CS-PEI block-copolymer formation,[17] CS labeling,[18] *etc.*) have recently been proposed as a means to modify the CS properties without compromising its ability to bind oppositely charged macro-ions such as nucleic acids. Two different CS attachment sites have been explored to date: the first is formed after CS depolymerization by nitrous acid (HONO) where a 2,5-anhydro-D-mannose unit (M-Unit) is formed at the reducing end of the cleaved polymer (Fig. 1, reaction 1), while the second site is available on the open-chain form, present in trace amounts, of the CS reducing extremity (either $GlcNH_2$ or GlcNHAc units) and allows mutarotation between the alpha and beta anomers. These coupling strategies thus rely on the reaction of the aldehyde moiety with nucleophilic species. However, in both cases, the aldehyde moiety appears to be mostly present in its hydrated and unreactive form (Fig. 1, reaction 2), also referred to as the *geminal-* or *gem*-diol form, under acidic aqueous conditions.[19–21]

The amines of CS in their neutral form are strong nucleophiles that can react with the aldehyde of CS's reducing end (Fig. 1 – reaction 3). Therefore block conjugation to the CS end-group requires that the proportion of CS amines in their reactive form be minimized, for example by performing reactions at pH significantly lower than the chitosan pK_a, typically near 6.5. However, chitosan pK_a varies with both ionic strength and CS charge density and can reach values as low as about 5.5 at high charge density and in the absence of added salt.[23] To date, all CS end-group conjugation reactions that have been implemented rely on oxime-click chemistry.[16,18,24,25] The oxyamine moieties involved in these studies have a pK_a value around 5 [26] and are therefore only slightly more reactive than CS amines in acidic aqueous conditions. Additionally, although the carbon–nitrogen double bond resulting from oxime-click chemistry is more hydrolytically stable than standard imino linkages,[27] a conjugate stabilization by an external chemical reagent (*e.g.*, hydrides) is necessary to stabilize the structure.[28] Moreover, it appears that CS conjugations with such chemistry usually require a polar aprotic co-solvent addition such as acetonitrile, DMF or DMSO to improve the reaction efficiency.[29]

The only slightly higher reactivity of oxyamine moieties towards CS aldehyde as compared to CS amines, along with the necessity of an external chemical treatment to stabilize the products and the requirement of an organic co-solvent addition, constitute limitations of the oxime-click pathway. These limitations could be overcome by a thiol-based chemistry. Indeed, thiol moieties are highly reactive towards double bonds as well as towards carbonyl groups in aqueous conditions at pH values as low as 1 where CS amines are present only in the ionized and non-reactive form.[30] Moreover, many equilibrium measurements have demonstrated the ability of thiols to add to the carbonyl group more efficiently than other nucleophiles (*e.g.*, hydroxyls or amines) in both acid- and base-catalyzed pathways.[31] Whereas amines produce Schiff base compounds (Fig. 1, reaction 3), thiols react with either aldehydes or ketones to produce hemithioacetals through a double equilibrium (Fig. 2). It is worth mentioning that the reactive species is the dehydrated carbonyl compound so that dehydration and hemithioacetal formation represent the rate-limiting steps of this pH-dependent process.[30,32]

Indeed, acid-catalyzed hemithioacetal formation takes place optimally below pH 3 [30] and the final product is unstable under

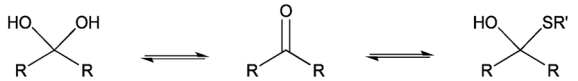

Fig. 2 Schematic representation of the equilibria involved in thiol-carbonyl additions.

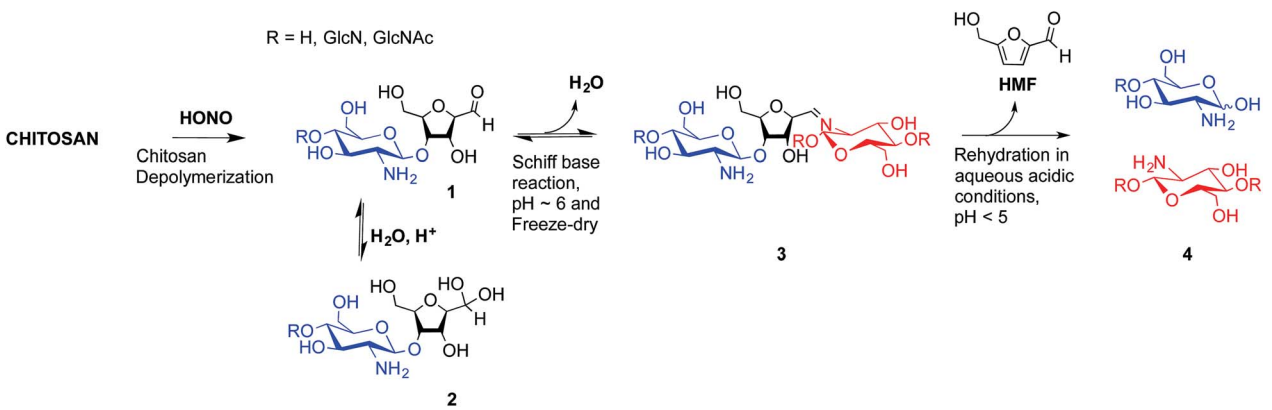

Fig. 1 Production of 2,5-anhydro-D-mannose unit (M-Unit) at the reducing end of chitosan by depolymerization in nitrous acid (HONO): chitosan depolymerization with nitrous acid (HONO) is a rapid, well-understood, and easily controlled method for producing chitosan harbouring a 2,5-anhydro-D-mannose unit (M-Unit) at the reducing end of the cleaved polymer.[22] A free aldehyde group (electrophile) is then potentially accessible (**1**) for reaction with nucleophilic moieties (*e.g.*, CS amine groups, thiols, oxyamines, *etc.*). Tømmeraas *et al.*[20] demonstrated that the M-Unit aldehyde also exists in its *gem*-diol hydrated form (**2**). The neutralization of CS and subsequent freeze-drying of the depolymerization medium induces a Schiff base formation between CS neutralized amines that react with the CS M-Unit aldehyde (**3**). The rehydration of the imino-adducts in acidic aqueous conditions cleaves the imino linkage between CS chains, transforming the M-Unit into hydroxymethylfurfural (HMF) (**4**).

alkaline conditions, since the attack of hydroxide ions readily reverts the product to the starting reactants.[33,34]

By analogy with Schiff base formation where amines and carbonyls react to give an imino linkage (Fig. 1, reaction 3) that needs to be stabilized by reduction, hemithioacetals can be stabilized by thioacetal formation *via* a second thiol nucleophilic attack (intra- or inter-molecular) associated with the release of water.[35] This chemical process is widely used in organic synthesis as a carbonyl group protection strategy; it is more conveniently performed in anhydrous organic solvent.[36] To the best of our knowledge, such a strategy has not been implemented yet in aqueous conditions for polymer derivatization.

The main objectives of the present study were to determine which form of the aldehyde predominates on the CS end-group (*i.e.* hydrated *vs.* dehydrated form for a CS depolymerized using HONO) and to assess its reactivity towards thiol moieties in aqueous conditions. NMR spectroscopy experiments were performed in order to assess the availability of the CS aldehyde end-group after HONO depolymerization, since this issue has not been clearly addressed. The mechanism of stabilization of hemithioacetals by conversion to their corresponding thioacetals was also investigated by liquid chromatography-mass spectrometry (LC-MS) analysis of the products of the reaction between mannose and two small thiol-bearing molecules, namely 3-mercaptopropionic acid (MPA) and β-mercaptoethanol (BME). This process was then examined by reacting MPA and BME with a CS bearing an M-Unit end in aqueous conditions. The conjugation efficiency was determined by a combination of NMR and Ellman assays. Finally, the PEGylation of the CS M-Unit aldehyde by thioacetylation was examined as a direct application of this conjugation strategy. Fig. 3 summarizes the objectives and the hypotheses of our study. Of interest, although the unreactive hydrated *gem*-diol M-Unit aldehyde moieties are predominant in acidic aqueous conditions, the thiol species react preferentially with this M-Unit *versus* CS amines post-HONO depolymerization, therefore avoiding the M-Unit cleavage after rehydration of the freeze-dried product. The conjugation between the M-Unit and thiol species is followed by stabilization of the hemithioacetal intermediate into the corresponding thioacetal by a second thiol nucleophilic attack. By analogy with the Schiff base formation, freeze-drying can thus be implemented to favour the present reaction by water removal.

Materials and methods

Each chemical reaction was performed on at least three independent occasions ($N = 3$), in Ar degassed ddH_2O and fresh reactants to minimize disulfide bond formation.

Reagents, materials

Chitosan with a degree of deacetylation (DDA) of 91.7%, M_n = 193 kg mol^{-1} (PDI = 1.256) and 99.5%, M_n = 0.8 kg mol^{-1} (PDI = 1.245) was provided by Marinard Biotech Inc. Deuterium oxide (Cat #151882), deuterium chloride 35 wt% in deuterium oxide (Cat #543047), sodium nitrite (Cat #431605), hydrochloric acid standard solution 1.0 M in H_2O (Cat #31894-9), hydrochloric acid 37% (Cat #320331), sodium hydroxide solution 1.0 M (Cat #319511), sodium acetate (Cat #241245), DTNB (5,5′-dithiobis-(2-nitrobenzoic acid)) (Cat #D8130), $GlcNH_2$ D-(+)-glucosamine hydrochloride 99% (Cat #C-1276), MPA (3-mercaptopropionic acid) ≥99% (Cat #63768), BME (β-mercaptoethanol) (Cat #M6250), sodium acetate trihydrate BioXtra (Cat #S7670), Dowex® 50WX8-100 [H^+] (Cat #217506), Dowex® 1X8-50 [Cl^-] (Cat #217417) and sodium azide (Cat #S2002) were purchased from Sigma-Aldrich. UltraPure™ TRIS (Cat #15504-020), glacial acetic acid (Cat #351271-212) and Spectra/Por®6 dialysis membrane (MWCO = 1000 Da, Cat #132640) were purchased from Life Technologies, Fisher Scientific and Spectrum Labs respectively. *m*PEG–SH 2 kDa and the plasmid DNA (pDNA) pEGFPLuc were purchased from JenKem Technology USA and from Clontech Laboratories, respectively.

Aldehyde availability

Chitosan depolymerization using deuterated species for direct ^{1}H NMR measurements.[22] The depolymerization reaction was performed in deuterated solvent for direct M-Unit CS aldehyde detection by ^{1}H NMR spectroscopy without further processing post-reaction. Chitosan with 92% DDA and M_n = 200 kg mol^{-1} (CS 92-200) was depolymerized using nitrous acid in deuterated solvent to achieve a specific number-average molar mass (M_n) target of 1 kg mol^{-1} (CS 92-1). These short CS chains were used to facilitate the detection and the quantification of aldehyde end-groups. Chitosan (202.5 mg) was dissolved in 37.9 mL D_2O and 170 μL of DCl 35% (w/w) at 50 °C. Then 2.435 mL of fresh sodium nitrite solution (10 mg mL^{-1} in D_2O) was added to the dissolved CS to reach 0.5% (w/v) chitosan concentration. These conditions correspond to a $GlcNH_2$: HONO molar ratio of 3. The mixture was stirred for 3 h at 50 °C. The pD (pD = pH + 0.4)[37] of the depolymerization medium was *ca.* 1.9 at the end of the reaction.

^{1}H NMR (ESI S1†) (500 MHz, D_2O/DCl, 70 °C, ns = 2000, d_1 = 6 s, acquisition time = 2 s) δ 2.06 (s, 1.38*H*, NHAc), 3.13–3.19 (br, 4.5*H*, H2D), 3.49–3.51 (br, 1*H*, H2A), 3.73–3.95 (m, 27*H*, H3–H6), 4.12–4.13 (q, J = 5.1 Hz, 1*H*, H5M), 4.22 (t, J = 3.9 Hz, 1*H*, H4M), 4.44 (t, J = 3.9 Hz, 1*H*, H3M), 4.58 (br, 0.5*H*, H1A), 4.79–4.88 (m, 4.5*H*, H1D), 5.09 (d, J = 5.3 Hz, 0.98*H*, H1M *gem*-diol).

SEC-MALLS: M_n = 823 (±41) g mol^{-1}; M_w = 1024 (±28) g mol^{-1}; PDI = 1.245 (±0.027).

Thiol reactivity towards M-Unit CS aldehyde

Mechanistic evaluation of chitosan thioacetylation by mass spectrometry (Fig. 4A). The CS terminal end-group (2,5-anhydro-D-mannose) formed after HONO depolymerization was derivatized with thiol-bearing model molecules (BME and MPA). Since the expected products have similar structures, their sensitivity to ionization should be equivalent. These derivatized M-Unit products were analyzed in a semi-quantitative way by comparing the chromatogram integration peaks of specific m/z values corresponding to both proton ([M + H]$^+$ and sodium adducts [M + Na]$^+$) within the same run.

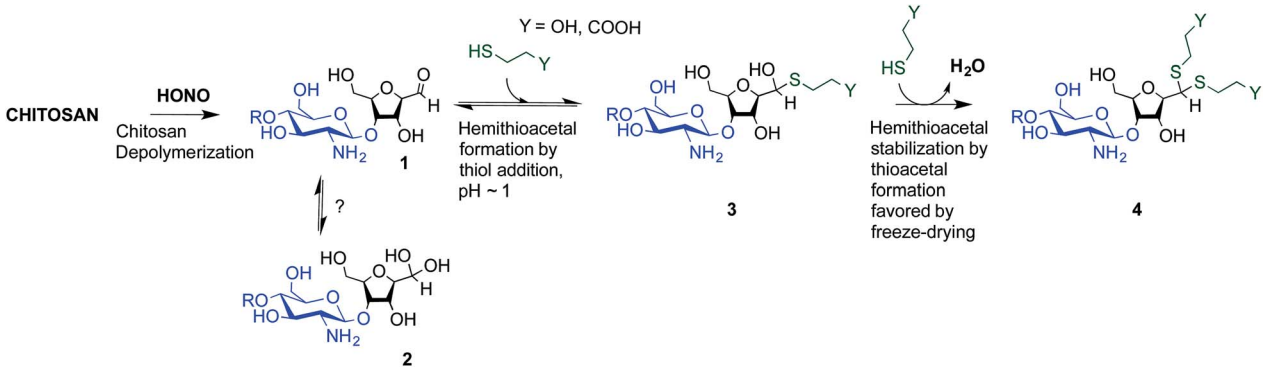

Fig. 3 Thioacetal conjugation to the chitosan M-Unit formed post-HONO depolymerization: the first objective of this study was to assess the availability of the reactive form of the unhydrated M-Unit aldehyde (**2**). Although there could be a strong displacement of the equilibrium towards the unreactive aldehyde-hydrated or *gem*-diol form in water, we hypothesized that efficient nucleophilic conjugation to the M-Unit was possible in acidic aqueous conditions. The second objective was to assess the M-Unit reactivity towards thiol moieties in aqueous conditions. The proposed reaction pathways between CS end-groups and thiols include the M-Unit CS aldehyde reacting directly with a thiol-bearing model molecule (β-mercaptoethanol and 3-mercaptopropionic acid, BME and MPA respectively) to form a hemithioacetal intermediate (**3**) through a pH-dependent equilibrium. By analogy with Schiff base formation where the equilibrium displacement occurs by water removal, the hemithioacetal can be stabilized into the corresponding thioacetal (**4**) by freeze-drying.

2,5-Anhydro-D-mannose (M-Unit) synthesis. 2,5-Anhydro-D-mannose was synthesized according to Claustre *et al.*[38] Briefly, $GlcNH_2 \cdot HCl$ (5 mmol, 1 g) was dissolved in 25 mL degassed ddH_2O and was allowed to stir overnight at room temperature. The colorless reaction medium was cooled down to 0 °C and $NaNO_2$ (12.5 mmol, 862 mg) was added. Dowex® 50WX8-100 [H^+] resin (42.5 mmol, 8.85 g dried, 25 mL) was added slowly under stirring and the heterogeneous mixture stirred for 4 h at 0–5 °C. The H^+ resin was removed by filtration and the filtrate was neutralized with Dowex® 1X8-50 [CO_3^{2-}] resin (60 mmol, 17.14 g dried, 50 mL), flash-frozen and freeze-dried to give the expected yellowish solid with 85% yield.

^{1}H NMR (500 MHz, D_2O, 25 °C, ns = 64, d_1 = 6 s, acquisition time = 2 s) δ 3.36–3.40 (m, 2*H*, H6), 3.91–3.95 (m, 2*H*, H2 & H5), 4.05–4.08 (t, J = 5.6 Hz, 1*H*, H4), 4.18–4.21 (t, J = 5.8 Hz, 1*H*, H3), 5.09–5.10 (d, J = 5.4 Hz, 0.88*H*, H1 *gem*-diol), 8.46 (s, 0.12*H*, H1 aldehyde).

MS (ESI$^+$): [M + H^+] = 163.0625; [M + Na^+] = 185.0460 (expected: [M + H^+] = 163.0601; [M + Na^+] = 185.0420).

2,5-Anhydro-D-mannose (M-Unit) conjugation with thiol-bearing molecules. The synthesized 2,5-anhydro-D-mannose M-Unit (0.1 mmol, 16.2 mg) was dissolved in 5 mL degassed ddH_2O. The pH of the solution was adjusted to 1 with 3 M HCl solution prior to the addition of the thiol-bearing molecule (0.5 mmol, 53.2 μL for MPA and 35.1 μL for BME). The pH was readjusted to 1 with 3 M HCl solution. The reaction mixture was stirred for 72 h at 25 °C, under Ar atmosphere and covered with aluminum foil. The reaction mixture turned clear pink-orange after 72 h and was split into 3 parts (Methods I, II and III): the first was dedicated to the direct LC-MS analysis of the reaction medium in order to determine the thioacetal proportion in resulting conjugates that formed *in situ*; the second one was directly flash-frozen and then freeze-dried prior to LC-MS analyses to assess the effect of FD (freeze-drying) on the thioacetal proportion in resulting conjugates and to ascertain that no by-products appear post-FD, whereas the third was treated with 1 M acetate buffer pH 4 before flash-freezing and freeze-drying in order to determine by LC-MS the effect of an increase in pH on the resulting conjugates. It is worth mentioning that Method III was included to prevent any CS acid hydrolysis that could occur when Method II, *i.e.* FD at pH 1, would be transposed to the polymer.

Characterization: mass spectrometry. Liquid chromatography-mass spectrometry (LC-MS) data were acquired using an Agilent 6224 LC-TOF mass spectrometer in positive electrospray ion mode, coupled to an Agilent 1260 series liquid chromatography system (Agilent Technologies). Mass Hunter B.06 software (Agilent Technologies) was used to process the data. Separations were carried out at 50 °C on an XSELECT CSH™ C18 column (4.6 × 100 mm, 5 μm particles) from Waters. The auto-sampler was maintained at 15 °C to avoid sample degradation. The eluents consisted of 0.1% formic acid in water (eluent A) and 0.1% formic acid in acetonitrile (eluent B). The initial mobile phase contained 1% eluent B and was held for 3 min. Eluent B content was increased from 1 to 20% from 3 to 5 min then from 20 to 80% from 5 to 7 min. The system returned to the initial conditions at 7.2 min and was held constant for up to 15 min to allow column equilibration. The injection volume was 1–3 μL. A needle wash solution containing methanol : water (60 : 40 v/v) was used after each injection to reduce carry-over. Mass spectra were acquired for *m*/*z* ranging from 50 to 1200.

Liquid chromatography coupled to tandem mass spectrometry (LC-MS/MS) experiments were performed using a Thermo Scientific Quantum Ultra triple quadrupole mass spectrometer operated in positive electrospray ion mode, equipped with a Thermo Scientific Surveyor liquid chromatography system. Xcalibur software (Thermo Scientific) was used to process the data. Separations were carried out on an XSELECT CSH™ C18 column (4.6 × 100 mm, 5 μm particles) from Waters operated under the same chromatographic gradients as those described above. MS/MS spectra were acquired on *m*/*z* values for protonated [M + $H]^+$ and sodium adduct [M + $Na]^+$ species of targeted compounds.

Chitosan end-group reactivity (Fig. 4B). Chitosan with 92% DDA and M_n = 200 kg mol^{-1} (CS 92-200) was depolymerized with nitrous acid (HONO) to a final molar mass of 2 kg mol^{-1} (CS 92-2). The final product was kept in its hydrochloride salt form by dialysis *vs.* HCl 1 mM solution and freeze-drying to minimize CS amines reacting with the M-Unit. This low 2 kDa molar mass was chosen in order to facilitate the elimination by dialysis of unreacted model thiols from the reaction mixture. The CS hydrochloride salt, carrying the 2,5-anhydro-D-mannose unit (M-Unit), was allowed to react at pH 1 with the two thiol models: 3-mercaptopropionic acid (MPA) and β-mercaptoethanol (BME). Each reaction was allowed to stir for 72 h, at two different temperatures (25 and 50 °C) under Ar atmosphere and were treated using three different workups: Workup I: dialysis *vs.* HCl 1 mM solution followed by freeze-drying (FD) to remove all thiol-bearing molecule excess and to determine the *in situ* thioacetal functionalization degree; Workup II: direct FD, dialysis *vs.* HCl 1 mM solution and a final FD to determine the effect of FD on the functionalization degree; Workup III: 1 M acetate buffer pH 4 addition to protect CS from acid hydrolysis during FD at pH 1, dialysis *vs.* HCl 1 mM solution and another FD to assess the effect of an increase in pH prior to FD on the functionalization rate. All conditions implemented are summarized in Fig. 4. Each final product was characterized by ^{1}H NMR, Diffusion Ordered Spectroscopy (DOSY) (5 mg mL^{-1} with 2% DCl in D_2O), SEC-MALLS (1 mg mL^{-1} in duplicates) and free thiol content was determined by Ellman assay (before and after Zn/HCl treatment to reduce any disulfide bond[39] that would not have been detected by the Ellman method). The following protocols describe the CS preparation as well as examples of the conjugation reactions performed in this study.

M-Unit CS 92-2 HCl salt synthesis. Chitosan was depolymerized using nitrous acid to achieve specific number-average molar mass targets (M_n) of 2 kg mol^{-1}. For depolymerization, chitosan (1 g) was dissolved in 184.5 mL ddH_2O and 9.54 mL HCl 1 M solution at 50 °C. Then 5.975 mL of fresh sodium nitrite solution (10 mg mL^{-1} in ddH_2O obtained by solubilization of 76.5 mg $NaNO_2$ in 7.65 mL ddH_2O) were added to the completely dissolved CS to reach 0.5% (w/v) chitosan concentration. These conditions correspond to a $GlcNH_2$: HONO molar ratio of 6. The viscous colorless mixture was stirred for 3 h at 50 °C. The reaction medium was then dialyzed 5× against 4 L of an aqueous solution of HCl at pH 3 (HCl 1 mM solution) over 2 days. The resulting colorless solution was flash-frozen with liquid nitrogen and freeze-dried over 3 days to give the desired white powder with 60–70% yield.

^{1}H NMR (500 MHz, D_2O, 70 °C, ns = 64, d_1 = 6 s, acquisition time = 2 s) δ 2.06 (s, 3.16*H*, NHAc), 3.14–3.21 (br, 13*H*, H2D), 3.51–3.56 (br, 1*H*, H2A), 3.68–3.95 (m, 70*H*, H3–H6), 4.12 (br, 1*H*, H5M), 4.21–4.31 (br, 1*H*, H4M), 4.43 (br, 1*H*, H3M), 4.61 (br, 1*H*, H1A), 4.87–4.89 (m, 13*H*, H1D), 5.08 (d, J = 5.0 Hz, 1*H*, H1M *gem*-diol).

SEC-MALLS: M_n = 2342 (±11) g mol^{-1}; M_w = 3117 (±4) g mol^{-1}; PDI = 1.332 (±0.008).

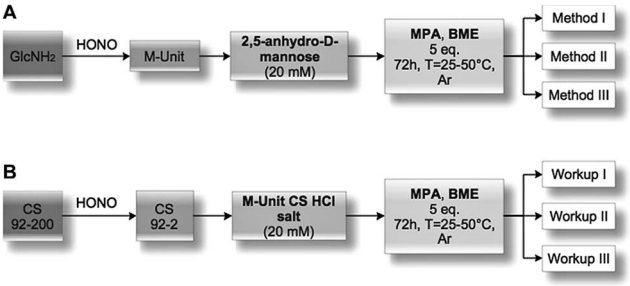

Fig. 4 Experimental design flowchart. (A) Mechanistic studies. Glucosamine ($GlcNH_2$) was treated with nitrous acid to form the 2,5-anhydro-D-mannose (M-Unit) that was reacted with 2 thiol-bearing molecules (β-mercaptoethanol and 3-mercaptopropionic acid, BME and MPA, respectively). The reaction products were treated using one of 3 methods, *i.e.* Method I: direct LC-MS analyses to determine to which extent thioacetal formation occurs *in situ*; Method II: freeze-drying (FD) + LC-MS analyses to assess the effect of FD on the thioacetal proportion and to ascertain that no by-products appear post-FD; Method III: acetate buffer pH 4 + FD + LC-MS analyses to determine the effect of an increase in pH prior to FD (this pH increase was included here to prevent any CS acid hydrolysis that could occur when Method II, *i.e.* FD at pH 1, would be transposed to the polymer). (B) Chitosan M-Unit reactivity. CS 92-200 was depolymerized with nitrous acid to produce CS 92-2 HCl salt bearing the M-Unit at the cleaved end of the polymer. M-Unit CS 92-2 HCl salt was reacted with MPA and BME and the reaction products treated with one of 3 workups: Workup I: dialysis *vs.* HCl 1 mM solution + FD to remove all thiol model excess and to determine the *in situ* thioacetal formation rate; Workup II: FD + dialysis *vs.* HCl 1 mM solution + FD to determine the effect of FD on the functionalization rate; Workup III: acetate buffer pH 4 + FD + dialysis *vs.* HCl 1 mM solution + FD to determine the effect of an increase in pH prior to FD on the functionalization rate (this pH increase was included to prevent any CS acid hydrolysis that could occur during FD at pH 1 in Workup II). The degree of functionalization of the CS conjugates was determined by ^{1}H NMR, whereas covalent conjugation was assessed by DOSY NMR experiments and Ellman assays in order to rule out the possibility of a simple physical mixture of reagents.

M-Unit CS 92-2 HCl salt conjugation with thiol-bearing molecules. CS 92-2 HCl salt (0.035 mmol, 70 mg) and thiol-bearing model molecules (0.175 mmol, 25.4 μL for MPA, 12.3 μL for BME) were solubilized in 1.73 mL degassed ddH_2O. The pH of the reaction medium was adjusted to 1 with 3 M HCl. The reaction medium was stirred for 72 h at either 25 or 50 °C under Ar atmosphere. The resultant colorless liquid was directly flash-frozen with liquid nitrogen and then freeze-dried over 3 days. The freeze-dried white solid was solubilized in 5 mL ddH_2O and dialyzed 5× against 2 L HCl 1 mM solution to remove unreacted thiols. The colorless solution was flash frozen and freeze-dried to give the expected white solid with typically 70–80% yield.

Addition of BME (ESI S2†): ^{1}H NMR (500 MHz, D_2O/DCl, 70 °C, ns = 64, d_1 = 6 s, acquisition time = 2 s) δ 2.06 (s, 5.89*H*, NHAc), 2.91–2.95 (br, 2.78*H*, BME_CH_2S), 3.17–3.21 (br, 20*H*, H2D), 3.51–3.53 (br, 1*H*, H2A), 3.69–3.95 (m, 105*H*, H3–H6), 4.12–4.14 (br, 1*H*, H5M), 4.24–4.25 (br, 1*H*, H4M), 4.57–4.59 (br, 1*H*, H3M), 4.61–4.62 (br, 1*H*, H1A), 4.91–4.92 (m, 20*H*, H1D), 5.08–5.09 (d, J = 5.0 Hz, 0.30*H*, H1M *gem*-diol).

SEC-MALLS: M_n = 3177 (±57) g mol^{-1}; M_w = 3680 (±66) g mol^{-1}; PDI = 1.160 (±0.003).

Addition of MPA (ESI S3†): ^{1}H NMR (500 MHz, D_2O/DCl, 70 °C, ns = 64, d_1 = 6 s, acquisition time = 2 s) δ 2.06 (s, 4.18*H*, NHAc), 2.74–2.77 (t, J = 7.1 Hz, 2.33*H*, MPA_CH_2–CO), 2.97–3.01 (q, J = 6.8 Hz, 1.78*H*, MPA_CH_2S), 3.15–3.24 (br, 17*H*, H2D), 3.51–3.56 (br, 1*H*, H2A), 3.69–3.95 (m, 91*H*, H3–H6), 4.11 (br, 1*H*, H5M), 4.21–4.23 (br, 1*H*, H4M), 4.55 (br, 1*H*, H3M), 4.62 (br, 1*H*, H1A), 4.87–4.92 (m, 17*H*, H1D), 5.08 (d, J = 5.0 Hz, 0.47*H*, H1M *gem*-diol).

SEC-MALLS: M_n = 3053 (±81) g mol^{-1}; M_w = 3564 (±48) g mol^{-1}; PDI = 1.182 (±0.016).

Ellman assays. Thiol-derivatized CSs were analyzed using the Ellman assay to assess the presence of free thiols within the products. Ellman stock solutions (50 mM sodium acetate, 2 mM DTNB) were prepared by dissolving 39.7 mg of Ellman reagent and 205.1 mg of sodium acetate in 50 mL double deionized water (ddH_2O). Tris 1 M dilution buffer was prepared dissolving 6.1 g of Tris in 50 mL ddH_2O and adjusting the pH to 8.0 using HCl 1.0 M standard solution. Thiol concentrations were measured in triplicate by mixing 50 μL of Ellman stock solution with 100 μL of Tris dilution buffer and 10 μL of sample solution. After 15 min the mixture was diluted by the addition of 840 μL of ddH_2O and the absorbance at 412 nm read using a microplate reader Tecan Infinite® M200. Thiol concentrations were calculated from a standard curve prepared using either MPA or BME and measurements were performed in triplicates in a 96-well plate using 150 μL sample volumes. The CS used as starting material was dissolved at the appropriate concentration for each sample and used as a blank. Both NaOH and Zn/HCl treatments of the CS adduct solutions were implemented on separate samples to determine the presence of hemithioacetal intermediates and any disulfide bond formation within the final product by the Ellman assay, respectively. Concentrated 1 M NaOH and 1 M HCl solutions were used to minimize changes in CS concentration. After 45–60 min constant agitation of the reaction media, Ellman assays were performed using 10 μL of alkali sample solution for NaOH treatment. Zn/HCl treated samples were obtained by adding few μL of 1 M HCl (to reach pH 1) and 5 equivalents of Zn dust per CS; the supernatants were analyzed after centrifugation (1000*g* for 1 min).

Characterization: NMR and SEC-MALLS. The deacetylation degree (DDA) of chitosan was determined by ^{1}H NMR spectroscopy as previously described[40] using a Bruker Avance 500 spectrometer equipped with a Bruker 5 mm BBFO probe. Cross-polarization magic-angle spinning (CPMAS) and Bloch-decay (BD) ^{13}C NMR spectra were collected on a Bruker Avance 600 instrument equipped with a Bruker 4 mm BL4 CPMAS probe and samples were spun at the magic angle (54.7°) at a rate of 10–12 kHz. Diffusion ordered spectroscopy experiments (DOSY) were conducted on a Bruker II 400 equipped with a Bruker Diff30 probe, using 32 gradients between 11.2 and 358.4 gauss per cm with a gradient pulse (δ) of 1 ms, a diffusion time (Δ) of 60 ms.

Molar mass of starting 92% DDA chitosan was determined by size-exclusion chromatography (SEC) as previously described.[41] Measurements were acquired using a gel permeation chromatography system equipped with an LC-20AD isocratic pump, SIL-20AC HT autosampler, and CTO-20AC oven (Shimadzu). This setup was coupled to the following detectors: Dawn HELEOS II multiangle laser light scattering, Viscostar II viscosimeter and Optilab rEX interferometric refractometer (Wyatt Technology Co.). The starting materials were eluted through two Shodex OHpak columns (SB-806M HQ and SB-805 HQ) connected in series with a mobile phase composed of 0.15 M acetic acid, 0.1 M sodium acetate, 0.4 mM sodium azide, 0.1 M NaCl, pH 4.5.[42] A dn/dc value of 0.214 (DDA = 92%) was used and the number and weight average molar masses (M_n and M_w) of the CS starting materials were found to be 193 kg mol^{-1} and 242.5 kg mol^{-1} respectively.

Modified CS (depolymerized CS and thiol-coupled CSs) were analyzed in SEC using the same conditions but with columns SB-806M HQ and SB-803 HQ that are more suitable for the analysis of low molecular weight chitosans.

Quantitation of CS derivatization efficiency: functionalization degree (F) calculations. The functionalization degrees (F) of each conjugation were calculated according to the following equations:

$$F = \frac{\frac{1}{\alpha}\sum\int \mathrm{H}_{\text{Thiol peaks}}}{\frac{1}{\beta}\sum\int \mathrm{H}_{\text{M-Unit peaks}}} \times 100 \quad (1)$$

where $\mathrm{H}_{\text{Thiol peaks}}$ refers to the well-defined proton peaks of the thiol-bearing molecule conjugated to CS and $\mathrm{H}_{\text{M-Unit peaks}}$ corresponds to the well-defined M-Unit characteristic proton peaks. Both integrations in eqn (1) are normalized to the number of protons used for the calculation, namely α and β for the thiol-bearing molecule and M-Unit, respectively.

According to the mechanistic studies on the M-Unit model presented below, the hemithioacetal intermediate is fully stabilized into the corresponding thioacetal (as shown in Fig. 3, reaction 4, and Fig. 5) after freeze-drying of the reaction mixture in acidic conditions, thus two thiol-bearing molecules per M-Unit CS salt were considered for the calculation of the functionalization degree (F). For MPA adducts, two well-defined peaks corresponding to –CH_2–S– and –CH_2–CO– protons (*i.e.* 8 protons) appear on the NMR spectra. However, for BME adducts, only the –CH_2–S– peak is visible on the spectra, in agreement with NMR spectrum simulation[43] that predicts that the –CH_2–CO– peak is hidden by the CS H3–H6 broad peaks.[40] Thus, α values of 4 and 8 in eqn (1) where used for BME and MPA, respectively. For the M-Unit, the well-defined peaks corresponding to H_4M and H_5M protons were used for integration and a β value of 2 was thus used in the equation. From the above considerations, eqn (1) can be rewritten as eqn (2) and eqn (3) for BME and MPA conjugates, respectively:

$$F_{\text{BME}} = \frac{\frac{1}{4}\int \mathrm{H}_{\mathrm{CH_2-S}}}{\frac{1}{2}\int (\mathrm{H_4M} + \mathrm{H_5M})} \times 100 \quad (2)$$

$$F_{\text{MPA}} = \frac{\frac{1}{8}\left(\int \mathrm{H}_{\mathrm{CH_2-S}} + \int \mathrm{H}_{\mathrm{CH_2-CO}}\right)}{\frac{1}{2}\int (\mathrm{H_4M} + \mathrm{H_5M})} \times 100 \quad (3)$$

where the protons used for integration are defined in Fig. 5, for purified BME and MPA chitosan adducts.

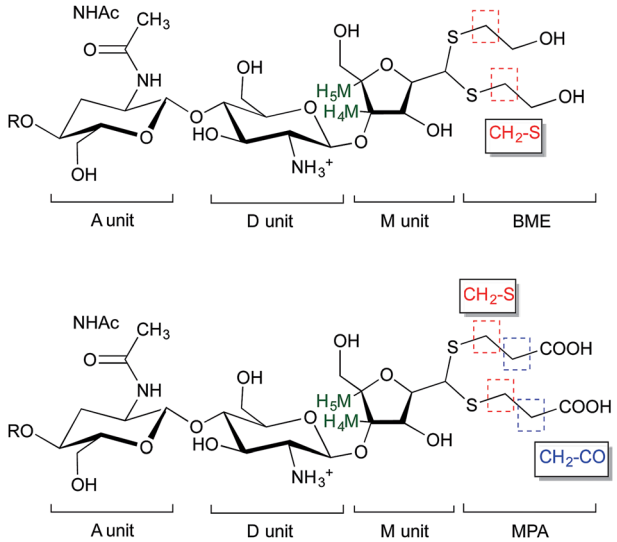

Fig. 5 Structure of BME (top) and MPA (bottom) chitosan adducts. The protons corresponding to the ^{1}H NMR peaks used for the calculations of the functionalization degree in eqn (2) and eqn (3) are highlighted.

Similarly, the CS PEGylation efficiency (F_{PEG}) was also calculated by adapting eqn (1) with the PEG characteristic peak integrations:

$$F_{PEG} = \frac{\frac{1}{6}\int H_{PEG-OCH_3}}{\frac{1}{2}\int (H_4M + H_5M)} \times 100 \quad (4)$$

where $H_{PEG\text{-}OCH_3}$ refers to the well-defined methyl proton (3H) peaks located at the end of the PEG chain ($\alpha = 6$ as there are 2 PEG chains per CS).

CS-*b*-PEG$_2$ block-copolymer

CS-*b*-PEG$_2$ block-copolymer formation. In order to reduce any *m*PEG–SS–PEG*m* disulfide bonds, *m*PEG–SH (2 kDa, m = 200 mg, 0.1 mmol) was solubilized in 2 mL Zn/HCl pH 1 solution (m(Zn) = 9.8 mg, 0.15 mmol) and the *m*PEG–SH solution stirred for 1 h. The clear colorless reduction medium was centrifuged at 1000*g* for 2 min prior to CS conjugation.

M-Unit CS 92-10 HCl salt (m = 100 mg, 0.01 mmol, 5 mM aldehyde) was added to the reduced *m*PEG–SH solution and the pH of the reaction medium was adjusted to 1 with HCl 3 M solution. The reaction medium was stirred for 72 h at 50 °C, under Ar atmosphere. At the end of the reaction, the reaction medium was flash-frozen and freeze-dried. Unreacted *m*PEG–SH was discarded by reprecipitation in 5 × 45 mL CH_2Cl_2. The remaining white pellet was dried under reduced pressure overnight.

^{1}H NMR (Fig. 8) (500 MHz, D_2O, 70 °C, ns = 64, d_1 = 6 s, acquisition time = 2 s) δ 2.06 (s, 11*H*, NHAc), 3.14–3.22 (br, 46*H*, H2D), 3.37 (s, 3.67*H*, PEG-OCH_3), 3.51–3.56 (br, 3*H*, H2A), 3.69 (s, 181*H*, PEG Chain –O–CH_2–CH_2), 3.75–3.95 (m, 238*H*, H3–H6), 4.12–4.14 (br, 1*H*, H5M), 4.21–4.23 (br, 1*H*, H4M), 4.61 (br, 3*H*, H1A), 4.88–4.90 (m, 46*H*, H1D), 5.08 (d, J = 5.0 Hz, 0.49*H*, H1M *gem*-diol).

CS-*b*-PEG$_2$ and CS/pDNA polyplexes formation. Polyplexes were prepared as previously described.[44] Briefly: CS-*b*-PEG$_2$ and depolymerized unmodified chitosan (CS 10 kDa with 92.5% DDA) stock solutions were prepared by dissolution at 0.5% (w/v) in hydrochloric acid using a glucosamine : HCl ratio of 1 : 1. Polymer stock solutions were diluted with ddH_2O to reach the amine to phosphate ratio of 3.7 (N/P = 3.7) when equal volumes of chitosan and pDNA (100 μg mL^{-1}) solutions would be mixed. Both CS-*b*-PEG$_2$/pDNA and CS/pDNA polyplexes were prepared at room temperature, by adding 100 μL of the diluted polymer solution to 100 μL of the pDNA solution followed by immediate mixing by pipetting up and down. The polyplexes were analyzed for their size and morphology by dynamic light scattering (DLS) and environmental scanning electron microscopy (ESEM) 1 h after their formation.

Polyplex characterization. Average diameters (*Z*-Average) of chitosan/pDNA and CS-*b*-PEG$_2$/pDNA polyplexes were determined by dynamic light scattering (DLS) at an angle of 173° at 25 °C, using a Malvern Zetasizer Nano ZS (Malvern, Worcestershire, UK). Samples (N = 2) were measured in triplicate using the viscosity of pure water in calculations.

Environmental scanning electron microscopy (ESEM) imaging of the polyplexes was performed as previously described[45] using an environmental scanning electron microscope, Quanta 200 FEG (FEI Company Hillsboro, OR), operated in high vacuum mode with accelerating voltage = 20.0 kV; spot size = 3 and working distance = 5 mm.

Results and discussion

Aldehyde availability

Since hemithioacetal formation requires the dehydrated aldehyde as reactive species (referred to as aldehyde in this manuscript), the CS aldehyde availability was assessed by NMR spectroscopy.

Chitosan 2,5-anhydro-D-mannose unit (M-Unit) – *gem*-diol ubiquity. Raw CS was depolymerized using HONO to a final molar mass of 1 kg mol^{-1} (CS 92-1). This low M_n was chosen to increase the concentration of aldehyde moieties, facilitating their detection by ^{1}H NMR spectroscopy. The use of deuterated solvent for the depolymerization reaction in this study allowed direct NMR analysis of the reaction mixture (ESI S1†). In the ^{1}H NMR spectrum, no aldehyde group was observed either at 9–9.5 ppm (the expected aldehyde proton chemical shift), or at 8.5 ppm (for the M-Unit model) despite the use of a large number of scans (2000). However, its hydrated form, the *gem*-diol peak at 5.09 ppm was omnipresent within the reaction medium. It is worth mentioning that the absence of the dehydrated form in the NMR spectrum is not due to a fast exchange between the hydrated and dehydrated forms since both forms were detected for the 2,5-anhydro-D-mannose (M-Unit).

Equilibrium is strongly displaced towards the *gem*-diol form for the M-Unit CS. The hydrated form of the aldehyde was the only form detected in each liquid NMR analysis, either at 25 °C (data not shown) or 70 °C (ESI S1†). It is worth mentioning that these analyses were performed in D_2O and/or D_2O/DCl, which are favorable conditions for the hydrated form or *gem*-diol

formation.[46] Some authors also reported an increase in the acetaldehyde carbonyl hydration equilibrium constant (K_{hyd} = [*gem*-diol]/[aldehyde]) from 0.85 to 0.99 when experiments are performed in ddH_2O and D_2O respectively, showing that the equilibrium can be displaced towards the formation of *gem*-diol in deuterated solvents.[30,46] In order to eliminate the contribution of the aqueous solvent on this equilibrium and to favor a displacement towards the aldehyde or unhydrated form of the CS end unit, 1 kg mol^{-1} M-Unit CS HCl salt was analyzed by solid-state NMR (CP-MAS). Fully deacetylated CS (CS 99-1) was preferred to the CS 92-1 to avoid any confusion between the carbonyl chemical shift of the acetyl peak and the aldehyde peak. The same sample was analyzed at two different frequencies (10 kHz and 12 kHz) to detect the eventual presence of harmonics within the spectrum. All peaks corresponded to chemical moieties attributed according to Heux *et al.*[47] (data not shown). The CS salt did not form any Schiff base product, as expected (since protonated amines are not nucleophilic); however, no aldehyde peak was detected in these spectra.

It has been reported that hydration of an aldehyde in the gas-phase can be observed at a relative humidity (RH%) level as low as 5%.[48] The relative humidity of the laboratory where the experiments were performed was between 20 and 50%, and it could be that all aldehyde groups were transformed into *gem*-diols during the sample transfer and preparation. To eliminate the exposure to air humidity that might favor this formation of the *gem*-diol, an inert atmosphere solid-state NMR experiment was implemented on an extra-dried CS 99-1 salt (freeze-dried over 3 days and then dried using a Speed-Vac Plus centrifuge at 60 °C, overnight under reduced pressure). Sample preparation was performed within an Ar glove box to verify if air humidity transforms the CS terminal aldehyde into its corresponding hydrate. The solid-state NMR analysis was conducted under an inert atmosphere as well (constant N_2 flow). Neither the aldehyde peak (expected around 190 ppm)[49] nor the *gem*-diol peak (expected around 90 ppm)[20] were visible on the spectrum. It is worth mentioning that the expected chemical shift of the *gem*-diol falls within the range of chemical shifts corresponding to C3–C5 peaks and the former is most probably hidden by the latter (ESI S4†). In order to confirm that the absence of the *gem*-diol in the spectrum was not due to an unexpected side reaction occurring in the preparation of the chitosan sample, the dried sample was subsequently dissolved in D_2O and analyzed by standard ^{1}H NMR. This analysis revealed that the hydrated aldehyde form was present at the expected quantitative proportion, as established from CS M_n and DDA values (data not shown).

H-bonding could stabilize the M-Unit CS *gem*-diol. Although for most aldehydes and ketones the hydrates are generally less stable than their respective parent,[46] their equilibrium can be displaced towards the *gem*-diol form by making the carbonyl more electropositive. Thus, the *gem*-diol form can predominate when the aldehyde is located close to a functional group allowing a negative inductive effect. For CS, some suitable electron-withdrawing substituents, such as hydroxyl and hemiacetal substituents might create a weak negative inductive effect, thereby increasing slightly the δ^+ charge on the carbon of the carbonyl and favouring water nucleophilic attack. Since CS offers significantly more H-bond donors than 2,5-anhydro-D-mannose, intermolecular H-bonding may be responsible for the strong predominance of the *gem*-diol form.[50] This hypothesis was confirmed with the ^{1}H NMR analysis of the synthesized 2,5-anhydro-D-mannose that presents a detectable proportion of the aldehyde in ^{1}H NMR spectroscopy (around 10% of the aldehyde form, data not shown). The NMR experiments described above suggest that the M-Unit CS aldehyde is only present in trace amounts since only the *gem*-diol form was detected. Nonetheless these trace amounts are reactive enough to be engaged with nucleophiles such as CS amines (Schiff base formation) or more particularly with thiol moieties (Fig. 1 and 3).

Mechanisms of conjugation of 2,5-anhydro-D-mannose (M-Unit) and thiol-bearing molecules

The reactivity of aldehydes toward thiols in aqueous conditions was assessed semi-quantitatively by LC-MS using the 2,5-anhydro-D-mannose as an aldehyde model.

Expected products of thiol conjugation to aldehydes include hemithioacetal, thioacetal, oxathiolane and α,β-unsaturated sulfide intermediate. The expected products of all conjugations implemented with thiol-bearing molecules (MPA and BME) include hemithioacetal, thioacetal, oxathiolane and α,β-unsaturated sulfide intermediate (Fig. 6). The first thiol attack on the aldehyde forms a hemithioacetal intermediate (**A**), which is in equilibrium with its corresponding protonated hemimercaptal form (oxonium) *via* a proton transfer. This structure may react in several ways: it could be stabilized with a second nucleophilic attack forming the corresponding thioacetal (**C**) after water removal; another hypothetical pathway is the formation of an α,β-unsaturated sulfide intermediate (**D**) through an elimination process; the final possible product concerns the BME adducts that could form oxathiolane-derivatized adducts (**B**), but this possibility is slight given their fast hydrolysis compared to the thioacetal.[51,52]

Low *in situ* stabilization of hemithioacetals. Five equivalents of thiolated molecules (BME and MPA) per M-Unit aldehyde/*gem*-diol were reacted with a synthesized 2,5-anhydro-D-mannose (M-Unit model) for 72 h at pH 1, under inert atmosphere. The relative proportions of the final expected compounds were calculated from LC-MS chromatogram integrations of specific *m*/*z* values corresponding to both proton and sodium adducts ($[M + H]^+$ and $[M + Na]^+$) within the same run (Table 1). This semi-quantitative evaluation was possible since the expected final products have similar structures and thus expected similar ionization behaviors. Direct LC-MS analyses (Table 1) of the reaction media (Method I, Fig. 4) indicated that the hemithioacetal intermediate **A** corresponded to the major observed compound (75%), the minor product being the stable thioacetal **C** (25%), after 72 h reaction. A highly similar 4 : 1 ratio of hemithioacetal to thioacetal was observed for all thiol models (BME and MPA) tested. Thus the stabilization to the thioacetal intermediate **A** seems to occur with a second thiol nucleophilic attack to form the corresponding thioacetal **C** with

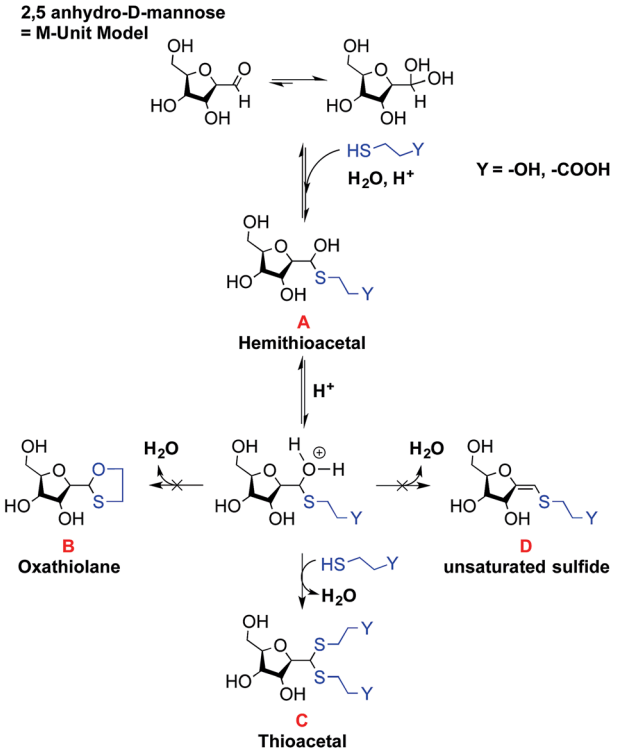

Fig. 6 Schematic representation of potential reactions occurring during conjugation of 2,5-anhydro-D-mannose (M-Unit) and 2 thiol-bearing models (3-mercaptopropionic acid and β-mercaptoethanol, MPA and BME respectively) giving the following expected products: product **A** is the hemithioacetal intermediate that is in equilibrium with its corresponding oxonium, whereas products **B** and **C** correspond to the oxathiolane (for BME reactions only) and thioacetal, respectively. Molecule **D** represents the α,β-unsaturated sulfide. The results of this study suggest that the thioacetal **C** corresponds to the only stable form observed after freeze-drying.

the release of water. However, our results suggest that this stabilization occurs only to a relatively low extent in aqueous medium.

Freeze-drying facilitates the hemithioacetal stabilization. Water removal by freeze-drying (FD) is the key-step in Schiff base formation occurring between CS amines and CS terminal aldehyde.[20] A similar effect might be at play in the reaction with thiolated species. In order to assess whether or not FD could favor a second thiol nucleophilic attack to stabilize the structure, Method II (direct FD of the reaction medium, Fig. 4) was implemented. This strategy resulted in the synthesis of the thioacetal **C** without any detectable quantity of hemithioacetal **A**, as deduced from LC-MS analysis. These trends were also observed using Method III (increase in pH with 1 M acetate buffer pH 4 followed by FD, Fig. 4), initially proposed to prevent any CS acid hydrolysis that could occur when this method would be transposed to the polymer CS. Reaction mixtures that were treated this way resulted in a significant increase, when compared to Method I, of the relative proportion of stabilized thioacetal **C** *vs.* hemithioacetal **A**, corresponding to 96% and 82% thioacetal **C** for BME and MPA respectively (Table 1).

It is worth mentioning that the LC-MS analyses only provide the relative proportion of observed species so that similar results obtained with both Methods II and III do not necessarily corresponds to equivalent absolute conversion rates. For instance, since the hemithioacetal formation equilibrium is pH-sensitive[33] (increase in pH is known to displace the equilibrium towards the starting materials), the increased relative proportion of thioacetal **C** observed with Method III *vs.* Method I could be due to a reduction of the absolute amount of hemithioacetal **A** in the reaction mixture. The conversion degrees or functionalization degrees are calculated below by ^{1}H NMR of the purified conjugated polymers.

The oxathiolane **B** and α,β-unsaturated sulfide products **D** appeared as traces in both Methods II and III (Table 1). LC-MS chromatograms revealed the same elution time as for thioacetals **C**, suggesting an in-source decomposition of **B**/**C** into their respective **D** form. The hypothesis that the oxathiolane **B** was formed within the MS apparatus by the ionization of the thioacetal **C** was confirmed by LC-MS/MS analyses of the **C**

Table 1 Expected product (Fig. 6) proportions as deduced from LC-MS analyses. Percentages represent the relative proportion of expected final molecules resulting from each conjugation that were implemented in triplicates ($N \geq 3 \pm$ SD): (**A**) hemithioacetal intermediate, (**B**) oxathiolane (for β-mercaptoethanol only), (**C**) thioacetal, (**D**) α,β-unsaturated sulfide. Calculations are based on chromatogram peak integrations of both proton and sodium adducts of a specific chemical formula. The *m*/*z* value given in parentheses represents the thioacetal in-source decomposition observations. Method I refers to direct LC-MS analysis of the reaction medium; Method II corresponds to the direct freeze-drying (FD) of the reaction medium before analysis; Method III corresponds to an increase in pH with acetate buffer pH 4 followed by FD. With both models, the hemithioacetal intermediate is stabilized by FD into the corresponding thioacetal. LC-MS/MS experiments rule out the possible formation (post-FD) of both oxathiolane and α,β-unsaturated sulfide (**B** and **D** forms in Fig. 6, respectively)

Model	Final product (see Fig. 6)	Chemical formula	Expected *m*/*z*		Observed *m*/*z*		Relative proportion (%)		
			$[M + H]^+$	$[M + Na]^+$	$[M + H]^+$	$[M + Na]^+$	Method I	Method II	Method III
M-Unit + BME	**A**	$C_8H_{16}O_6S$	241.0740	263.0560	—	263.0550	75 ± 13	—	4 ± 3
	B and **D**	$C_8H_{14}O_5S$	223.0635	245.0454	—	(245.0450)	—	—	—
	C	$C_{10}H_{20}O_6S_2$	301.0774	323.0590	301.0884	323.0577	25 ± 13	100	96 ± 3
M-Unit + MPA	**A**	$C_9H_{16}O_7S$	269.0689	291.0509	—	291.0502	76 ± 3	—	18 ± 7
	C	$C_{12}H_{20}O_8S_2$	357.0672	379.0492	—	379.0483	24 ± 3	100	82 ± 7
	D	$C_9H_{14}O_6S$	251.0584	273.0403	(251.0563)	(273.0386)	—	—	—

adduct obtained from the reaction of the M-Unit and MPA: the fragmentation of **C** produced compound **D** (data not shown).

These experiments suggest that the oxonium intermediate (which is in equilibrium with the hemithioacetal intermediate) is stable enough to favor the thioacetal formation notwithstanding the unsaturated compound **D** formation. The freeze-drying step apparently orients the reaction towards the stable thioacetal formation, more likely due to an increase in concentration by water removal to facilitate the second nucleophilic attack.

M-Unit chitosan HCl salt reactivity

Chitosan HCl salt maintains the M-Unit integrity after freeze-drying. The 2,5-anhydro-D-mannose unit (M-Unit) resulting from CS depolymerization using HONO is not stable after rehydration in aqueous acidic conditions. Indeed, when the reaction medium is neutralized, the reaction between CS amines and the M-Unit aldehyde moiety produces a reversible imino bond (Schiff base formation), which is accompanied with the release of water (Fig. 1, reaction 3). It has been demonstrated that after FD, which is accompanied by Schiff base formation *via* equilibrium displacement, the solubilization of CS in acidic conditions (pH below 5) cleaves 2,5-anhydro-D-mannose unit from CS into hydroxymethylfurfural (HMF)[20] (Fig. 1, reaction 4). In terms of reactivity, the M-Unit is available within the reaction medium after HONO treatment but its concentration is limited to that of the depolymerization medium (0.5% w/v in our case, corresponding to a concentration of reactive units of 2.5 mM for CS with $M_n = 2$ kg mol^{-1}). Higher CS depolymerization concentrations are possible (typically up to 2% w/v for CS with M_n of a few hundreds of kg mol^{-1}) but are limited by the high viscosity of the CS solutions, which may compromise the stirring efficiency and homogeneity of the depolymerization medium. In order to maintain the M-Unit integrity and to work in a more concentrated regime, the depolymerized (*i.e.* less viscous) CS hydrochloride salt was freeze-dried, with all CS amines protonated, thus avoiding Schiff base formation and subsequent HMF formation upon rehydration. All the CSs that were prepared this way still carried their M-Unit after rehydration (M-Unit remaining $\geq$ 80%), allowing higher CS concentration than the depolymerization medium (4% w/v *vs.* 0.5% w/v, respectively).

The covalent nature of the conjugation of the CS HCl salt M-Unit to thiol-bearing molecules was confirmed by the Ellman assay where no free thiol moieties were detected after rehydration of the modified polymers. Note that free thiol moieties were not detected after Zn/HCl treatment that would have reduced any disulfide bond potentially formed in the course of the conjugation reaction and/or post-reaction workup. The absence of any hemithioacetal intermediate (base-sensitive) was also confirmed by performing the Ellman assay on the product after exposure to 1 M sodium hydroxide solution. Purified CS-thiol adducts were also analyzed by diffusion ordered spectroscopy (DOSY), a spectroscopic method that distinguishes compounds according to their respective translation diffusion coefficient (ESI S5†), shows that both CS and thiol-bearing models have the same diffusion coefficient in D_2O at 25 °C, despite significant molar mass differences (2300 g mol^{-1} *vs.* 106 g mol^{-1}, for M-Unit CS HCl salt and MPA respectively). Altogether, the aforementioned controls confirmed the presence of the thioacetal linkage between the CS HCl salt M-Unit and both thiol-bearing model species. The results of the conjugation efficiencies between CS and BME or MPA were calculated using eqn (2) and (3) respectively and are summarized in Table 2.

NMR and LC-MS analyses indicate that two thiol-bearing molecules regioselectively react with the CS M-Unit aldehyde to form a thioacetal. The regioselectivity of the CS M-Unit aldehyde conjugation to the thiol models was assessed by 2D NMR experiments (COSY and HMBC, data not shown) in order to detect long-range correlations between the M-Unit and the thiol characteristic peaks. However, such correlations were not visible in the NMR spectra, most probably because of the inherently low concentration of the end-group conjugated thiols within the synthesized structures and/or because the atoms to correlate are separated by a large number of bonds (3 and 4 for proton–carbon and proton–proton correlation, respectively – see Fig. 5), especially for the COSY experiments.[53,54] Moreover, the HMBC measurements were found to be insensitive, particularly with poorly resolved ^{1}H–^{1}H multiplets (ESI S2 and S3†).[55,56]

Despite the inability of these 2D NMR experiments to reveal the expected correlations, the combined NMR and LC-MS analysis indicated that two thiol-bearing molecules react regioselectively with the aldehyde of the terminal M-Unit of chitosan. As discussed above, the MS experiments performed with the mannose monomer indicated clearly that the stabilized form is the thioacetal form, so that, two thiols are expected to react similarly with the M-Unit of chitosan. This expected stoichiometry and regioselectivity for thiol-bearing molecules reacting on chitosan was validated by monitoring the relative proportion of *gem*-diol. Indeed, the *gem*-diol signal should decrease concomitantly with the conjugation of thiols onto the M-Unit of chitosan (one *gem*-diol consumed for two conjugated thiols). The calculated conjugation efficiencies obtained with either eqn (2) (BME) or eqn (3) (MPA) and the following equation should therefore be the same if the two thiols react regioselectively onto the terminal aldehyde function of chitosan:

$$F = \frac{\frac{1}{2}\sum\int(H_4M + H_5M) - \int H_{gem\text{-diol}}}{\frac{1}{2}\sum\int(H_4M + H_5M)} \times 100 \qquad (5)$$

where H_4M and H_5M are protons with well-defined NMR peaks from the M-Unit shown in Fig. 5 (unchanged by the reaction of the aldehyde with thiol-bearing molecules) and $H_{gem\text{-diol}}$ is the H1 proton of the *gem*-diol form of CS M-Unit shown in ESI S1.† It is worth mentioning that efficiency calculation using eqn (5) is independent of the reaction stoichiometry and relies only on the assumption that any thiol-bearing molecule will react selectively with the terminal unit of chitosan.

For all conjugation reactions performed in this study, the conjugation efficiencies calculated with both approaches, namely with eqn (2) (BME) or eqn (3) (MPA), which both rely on the reaction stoichiometry, or eqn (5) that is independent from

Table 2 Efficiency of conjugation of the M-Unit CS HCl salt to 5 equivalents of thiol-bearing molecules (3-mercaptopropionic acid and β-mercaptoethanol, MPA and BME respectively) per CS end unit for 72 h at pH 1. Reaction media were treated according to the following workups: Workup I (dialysis *vs.* HCl 1 mM solution + FD); Workup II (FD + dialysis *vs.* HCl 1 mM solution + FD); Workup III (increase in pH with acetate buffer pH 4 + FD + dialysis *vs.* HCl 1 mM solution + FD). *F* below corresponds to the functionalization degree, considering 2 thiol molecules per potential aldehyde and calculated using eqn (2) for BME and eqn (3) for MPA with $N \geq 3$ (±SD). *F* was also calculated using eqn (5), considering only the relative proportion of the remaining *gem*-diol per M-Unit. (* corresponds to the results of the conjugations implemented with 20 equivalents (instead of 5) of thiol-bearing molecule per end unit)

		Workup I		Workup II		Workup III	
		F (%)	*F* (%)	*F* (%)	*F* (%)	*F* (%) eqn (2)	*F* (%)
Thiol-bearing molecule	Temperature (°C)	eqn (2) and (3)	eqn (5)	eqn (2) and (3)	eqn (5)	and (3)	eqn (5)
BME	25	2 (±1)	3 (±1)	18 (±2)	18 (±1)	11 (±2)	11 (±1)
	50	26 (±2)	24 (±1)	42 (±2)	42 (±3)	24 (±1)	24 (±0)
		68 (±1)*	69 (±1)*	70 (±1)*	70 (±1)*	—	—
MPA	25	10 (±1)	11 (±1)	18 (±2)	19 (±2)	15 (±1)	13 (±2)
	50	14 (±1)	13 (±1)	54 (±5)	55 (±2)	18 (±1)	17 (±1)
		56 (±1)*	55 (±1)*	59 (±1)*	58 (±1)*	—	—

stoichiometry and relies only on the relative proportion of *gem*-diol *vs.* M-Unit, were found to be in very close agreement (Table 2). These results indicate that (1) thiol-bearing molecules react selectively with the terminal aldehyde functional group of chitosan, and (2) the thioacetal is the only stable form of product observed.

The stabilization rate of the product from the hemithioacetal to thioacetal form within the reaction medium can be enhanced by FD. For reactions performed using 5 equivalents of thiol-bearing molecule per aldehyde, the first workup tested here (Workup I: dialysis *vs.* HCl 1 mM solution + FD) showed a limited conversion into the desired conjugates (F = 2% and 10% as conversion degrees, for BME and MPA at 25 °C respectively; Table 2). Similar results were obtained for Workup III (increase in pH with acetate buffer pH 4 + FD + dialysis *vs.* HCl 1 mM solution + FD) with F = 11% and 15% at 25 °C, for BME and MPA, respectively (Table 2), whereas significantly higher functionalization degrees were obtained for Workup II (FD + dialysis *vs.* HCl 1 mM solution + FD) where F = 18% at 25 °C, for both BME and MPA (Table 2). Similar trends were observed for reactions performed at 50 °C but with an overall increase in functionalization degrees (further discussed in the following section). These results suggest that FD favors the second thiol nucleophilic attack to stabilize the hemithioacetal structure, possibly by concentrating the reaction medium. This FD effect is only seen in Workup II since in Workup I, all thiol-bearing molecules were removed by dialysis prior to FD, whereas in Workup III, most of the hemithioacetal intermediate was readily transformed into the starting reactants by an increase in pH. Thus, one of the reacting species is absent (or present in very low amount) during the last FD step in Workup I (thiol-bearing molecule removed with concomitant hemithioacetal formation equilibrium displacement towards the starting reactants, Fig. 7) and Workup III (hemithioacetal intermediate amount reduced by pH increase) and the thioacetal form cannot be further increased by FD as compared to Workup II where both reacting species are present during FD. In fact, for Workup I and III, all observed thioacetals were mostly formed *in situ* during the 72 h reaction and results indicate that for reactions performed with 5 equivalents of thiol-bearing molecule per aldehyde, *in situ* stabilization into the thioacetal form is low.

Hemithioacetal-to-thioacetal conversion within the reaction medium is increased by large excess of thiol equivalents. The conjugations implemented with 20 equivalents of thiol-bearing molecules per CS end unit revealed higher conversion rates (F = 55–70% at 50 °C depending on the thiol-bearing molecules engaged) and were independent of the workup implemented (*i.e.* I and II, Table 2). These results also support the proposed reaction mechanism proposed in Fig. 7. Indeed, at higher thiol concentrations, hemithioacetal intermediates and thioacetal are both favored within the reaction medium. However, in this case, FD had no significant impact on the conversion degree. Our results suggest that at high thiol concentration (20 equivalents per aldehyde) the amount of thiol-bearing molecules is sufficient to achieve significant hemithioacetal stabilization *in situ*. The fact that FD has no significant impact on the functionalization rate is unclear and would require additional investigations.

Temperature favors both hemithioacetal formation and stabilization to the thioacetal form. The highest conversion degrees were obtained at 50 °C, regardless of the workup implemented (Table 2). Indeed, an increase in temperature

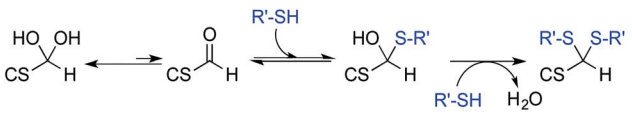

Fig. 7 Thiol addition to the aldehyde group of the M-Unit CS HCl salt under acidic aqueous conditions: despite the fact that the aldehyde is only present in trace amounts within the reaction medium, the pH-dependent hemithioacetal intermediate formation equilibrium can be displaced by the intermediate stabilization into the corresponding thioacetal at low thiol concentration.

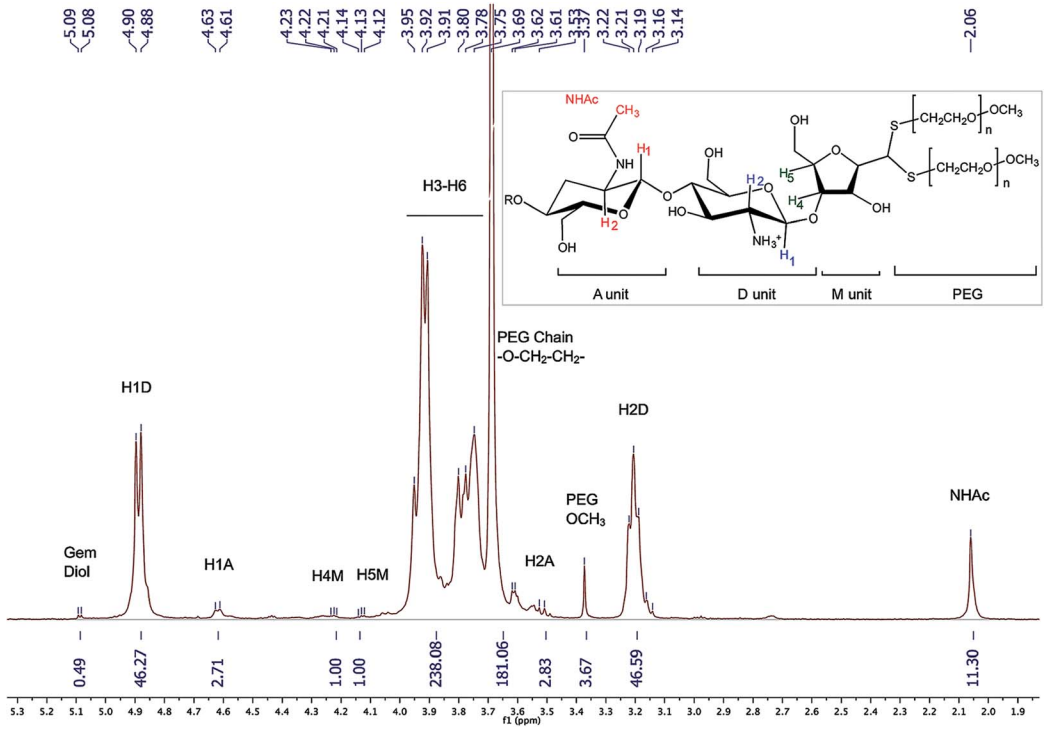

Fig. 8 ^{1}H NMR spectrum of the CS-*b*-PEG$_2$ block-copolymer after workup II (D_2O, $T = 70$ °C, HOD peak was presaturated, number of scans (ns) = 64, relaxation period (d_1) = 6 s, acquisition time = 2 s, exponential apodization = 1 Hz). Integration of *gem*-diol proton peak was used to calculate the functionalization degree (in this particular case, $F = 51\%$ according to eqn (5)).

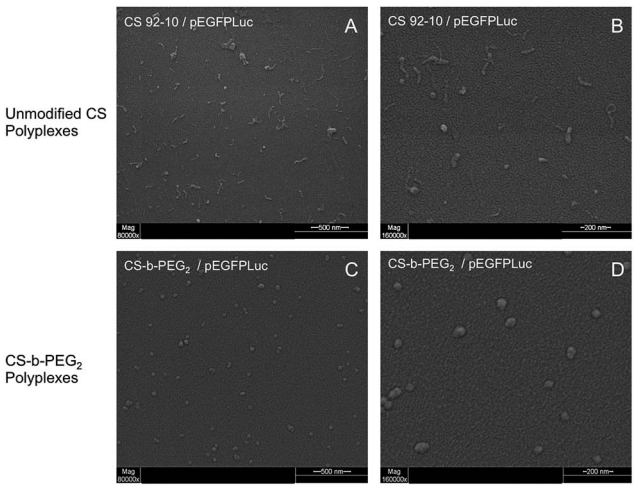

Fig. 9 Environmental scanning electron microscopy (ESEM) pictures (high vacuum mode, accelerating voltage = 20.0 kV; spot size = 3 and working distance = 5 mm) of polyplexes formed with pDNA and unmodified CS or CS-*b*-PEG$_2$ block-copolymer (amine to phosphate ratio = 3.7, N/P = 3.7). (A and B) (×80 000 and ×160 000, respectively): polyplexes formed with CS 92-10 are heterogeneous in size and present various morphologies (globular, rod-like and toroidal). Pictures C and D (×80 000 and ×160 000, respectively): polyplexes formed with CS-*b*-PEG$_2$ (CS 92-10 and *m*PEG–SH 2 kDa), are uniformly spherical.

favors the hemithioacetal intermediate formation by increasing the probability of thiol-bearing molecules to react with the CS HCl salt M-Unit aldehyde. Similarly, stabilization of the hemithioacetal intermediate occurred with an increase in temperature, favoring the second thiol model attack by increasing the probability of collisions between species. This mechanism is especially valid for the results corresponding to Workups I and III where no FD stabilization was reported. Indeed, the functionalization degree varied from 2 to 26% for BME and from 10 to 14% for MPA, for 25 and 50 °C respectively. The proposed mechanism involving an equilibrium between the starting reactants and the hemithioacetal intermediate (Fig. 7) is thus confirmed by this increase in conversion degree with temperature.

Effective CS PEGylation by thioacetylation of the CS M-Unit aldehyde

CS-*b*-PEG$_2$ block-copolymer synthesis. As a direct application of the thioacetylation conjugation developed in the paper herein, a 2 kDa *m*PEG–SH was reacted with a 10 kDa CS HCl salt. The choice of a 2 kDa PEG was based on the CS and PEG molecular weight (M_w) ratio (10 kDa and 2 × 2 kDa, respectively), expecting the PEG M_w to be large enough to form micellar structures (see section below). Because of solubility limitations with these longer chains, the reaction was performed at 5 mM aldehyde instead of 20 mM that was used for the reactions between the 2 kDa CS and MPA or BME. In order to counterbalance the decrease in aldehyde concentration, the reaction was performed at 50 °C for 72 h and ten thiol equivalents per aldehyde were used. After direct FD of the reaction medium and unreacted *m*PEG–SH removal by multiple

Table 3 DLS measurements of unmodified CS and CS-*b*-PEG_2 polyplexes prepared with pDNA (pEGFPLuc, N/P = 3.7). Samples were analyzed in triplicate ($N = 2$, ±(max − min)/2). The size of CS-*b*-PEG_2 polyplexes is smaller as compared to native polyplexes

Samples	*Z*-Average diameter/nm	PDI	Intensity-weighted mean diameter/nm
Unmodified CS polyplexes	106 (±8)	0.19 (±0.00)	131 (±11)
CS-*b*-PEG_2 polyplexes	76 (±5)	0.23 (±0.02)	96 (±11)

precipitations, ^{1}H NMR analysis of the final product (Fig. 8) was performed and functionalization degree values (*F*) of 61 and 51% were found with eqn (4) and (5) (where only the *gem*-diol peak integration decrease was considered), respectively.

The slight discrepancy between these two values could possibly be the due to the presence of residual *m*PEG–SH post-purification. This hypothesis was confirmed by SEC analysis of the conjugates, where a small residual peak identified as *m*PEG–SS–PEG*m* was detected. Because PEG and CS molecular weights are close to each other, the DOSY NMR processing used to validate covalent conjugation of MPA and BME to CS was found to be inefficient for the block-copolymer (data not shown).

CS-*b*-PEG_2 block-copolymer/pDNA polyplexes are homogeneously spherical. The CS-*b*-PEG_2 block-copolymer (CS 92-10 and 2 kDa *m*PEG–SH) synthesized above was used without further purification to form polyplexes with plasmid DNA (pEGFPLuc). Whereas ESEM imaging of polyplexes prepared with unmodified CS revealed various morphologies, namely

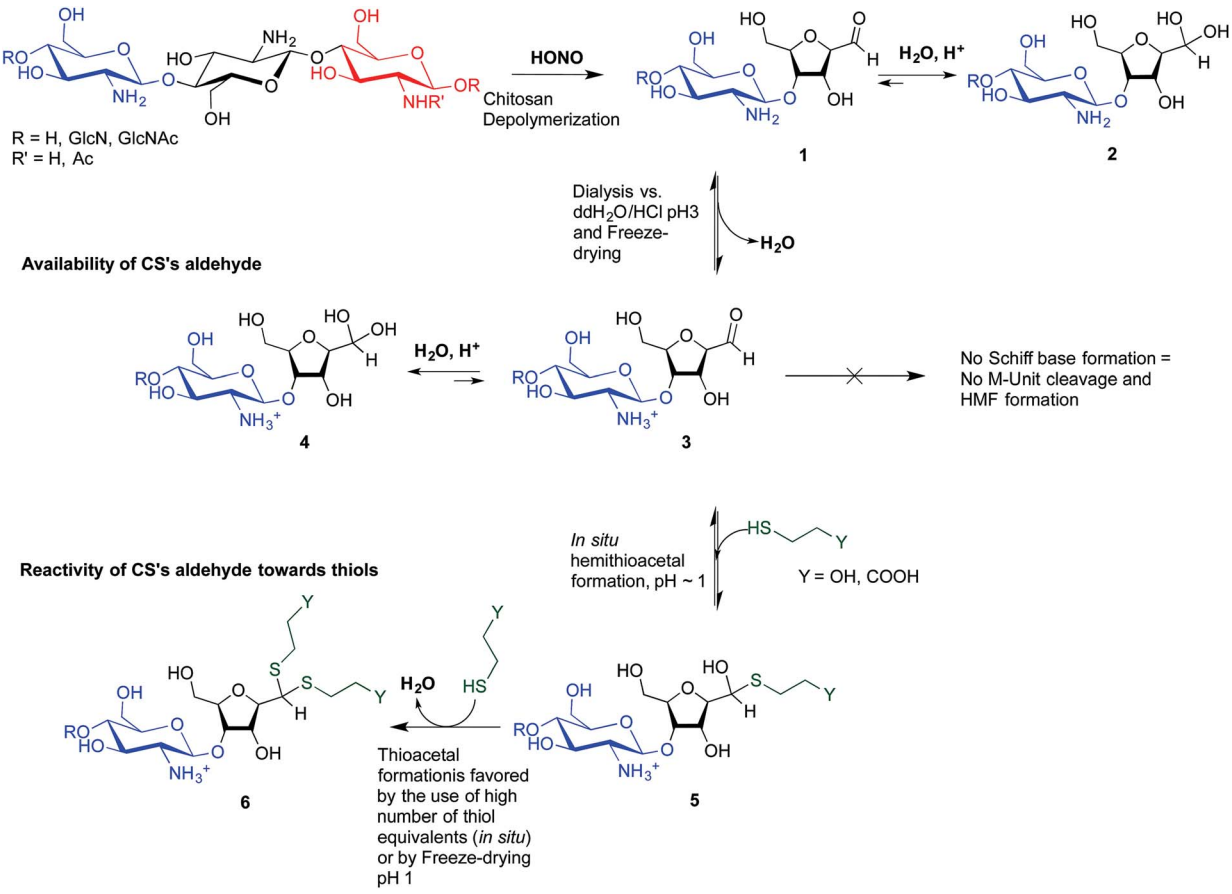

Fig. 10 Summary of mechanisms elucidated in this study for thiol-based end-group derivatization of chitosans: CS nitrous acid depolymerization induces the formation of M-Unit that carries an aldehyde moiety at the end of the cleaved polymer (**1**). The equilibrium between the M-Unit aldehyde and its hydrated form (*gem*-diol) is strongly displaced towards the latter (**2**). If the CS depolymerization medium is freeze-dried at pH well below the CS pK_a (*i.e.* pH ∼ 3–4 or below), all the CS amines are protonated and are therefore unable to react with any aldehyde group, maintaining the CS M-Unit integrity at the end of the cleaved polymer (**3**). Nevertheless, the equilibrium between the M-Unit aldehyde and the corresponding *gem*-diol is still displaced towards the hydrated form (**4**). Despite the undetectable aldehyde moieties, thiol molecules and the M-Unit CS aldehyde are engaged in a pH dependent equilibrium with the corresponding hemithioacetal intermediate (**5**). The stabilization of the latter into its thioacetal form (**6**) occurs either by increasing the amount of thiol-bearing reactants in the medium (*in situ* stabilization), or by freeze-drying the reaction medium when low amounts of thiol are engaged.

toroïds, spheres and rods, those prepared with CS-*b*-PEG_2 block-copolymer were uniformly spherical (Fig. 9). The structure modification of the polyplexes formed with PEGylated CS was also confirmed by DLS, where the measured *Z*-average diameters decreased from 106 (±1) to 76 (±1) nm, for the unmodified CS and CS-*b*-PEG_2 block-copolymer, respectively (Table 3).

Since the PEGylated polyplexes are uniformly spherical and show a narrower size as compared to those prepared with corresponding homopolyions, these observations are consistent with the formation of micellar structures called "Block Ionomer Complexes" (BICs).[57–59]

Conclusions

This study revealed that the aldehyde present on chitosan mannose (M-Unit) end-group is displaced completely towards its hydrated and unreactive form (*gem*-diol) in aqueous conditions. The ubiquity of the unreactive *gem*-diol form in aqueous conditions revealed by ^{1}H NMR (dehydrated reactive form not detected) could be due to both H-bonding and hydration effects. Despite the fact that the aldehyde reactive moiety is only present in trace amounts, the development and optimization of a thiol-based chemistry allowed efficient conjugation to the CS terminal M-Unit in aqueous conditions ($F = 55$–70% depending on the thiol-bearing molecule). A combination of mass spectrometry and NMR analyses revealed that two thiol-bearing molecules react regioselectively with the terminal aldehyde of the polymer to form a thioacetal. The stabilization of the hemithioacetal intermediate was found to be facilitated by freeze-drying (Fig. 10). As a direct application of this novel conjugation strategy, a CS-*b*-PEG_2 block-copolymer was successfully synthesized by thioacetylation of the CS 92-10 M-Unit aldehyde with a 2 kDa *m*PEG–SH. This block-copolymer was used to prepare polyplexes with pDNA that were found to be uniformly spherical and more homogeneous as compared to those prepared with native CS.

The new CS end-group thioacetylation process that was developed in this study presents several advantages in comparison to the oxime-click method developed previously.[16,18,24] That is (1) it can be used for CS derivatization without interfering with amine groups that are fully protonated and thus unreactive, (2) it is efficient in aqueous media, and (3) there is no need for an external chemical treatment to stabilize the adducts. It is worth mentioning that the stabilization of the hemithioacetal intermediate by a second nucleophilic attack could be sterically hindered by the presence of the first external group for large thiol-bearing substituents. In order to circumvent this issue and to further improve the conjugation efficiency, studies are ongoing where a molecule bearing two thiol groups (a thiol-based "hook") is used for conjugation to the CS M-Unit. The presence of two thiol moieties along with their adequate positioning on the molecule to be conjugated may allow for an intramolecular stabilization of the hemithioacetal, which is expected to rule out any steric hindrance issues and to occur *in situ* at significantly lower thiol concentrations *vs.* the intermolecular stabilization studied herein.

CS end-group modifications such as PEGylation and the formation of other types of block-copolymers as well as CS grafting onto surfaces *via* a single covalent bond are a few applications of our proposed green chemistry protocol. These could be advantageously applied to various biomedical research fields including gene delivery and tissue engineering. Additionally, we expect this thiol-based chemistry to be applicable to other polymers bearing aldehydes or ketones.

Acknowledgements

This work was supported by the Natural Sciences and Engineering Research Council of Canada (NSERC) and ANRis Pharmaceuticals. The authors would like to acknowledge Monica Iliescu Nelea (Polytechnique Montréal), Alexandra Furtos (Université de Montréal) and Cédric Malveau (Université de Montréal) for the ESEM pictures and helpful discussions on mass spectrometry and NMR spectroscopy, respectively.

Notes and references

1 M. Rinaudo, *Prog. Polym. Sci.*, 2006, **31**, 603–632.
2 H. Sashiwa and S.-I. Aiba, *Prog. Polym. Sci.*, 2004, **29**, 887–908.
3 I. Aranaz, R. Harris and A. Heras, *Curr. Org. Chem.*, 2010, **14**, 308–330.
4 L. Casettari, D. Vllasaliu, E. Castagnino, S. Stolnik, S. Howdle and L. Illum, *Prog. Polym. Sci.*, 2012, **37**, 659–685.
5 M. Garcia-Fuentes and M. J. Alonso, *J. Controlled Release*, 2012, **161**, 496–504.
6 M. D. Buschmann, A. Merzouki, M. Lavertu, M. Thibault, M. Jean and V. Darras, *Adv. Drug Delivery Rev.*, 2013, **65**, 1234–1270.
7 I. K. Park, T. H. Kim, Y. H. Park, B. A. Shin, E. S. Choi, E. H. Chowdhury, T. Akaike and C. S. Cho, *J. Controlled Release*, 2001, **76**, 349–362.
8 O. Germershaus, S. Mao, J. Sitterberg, U. Bakowsky and T. Kissel, *J. Controlled Release*, 2008, **125**, 145–154.
9 C. Zhang, Q. Ping, Y. Ding, Y. Cheng and J. Shen, *J. Appl. Polym. Sci.*, 2004, **91**, 659–665.
10 J. You, F. Q. Hu, Y. Z. Du and H. Yuan, *Biomacromolecules*, 2007, **8**, 2450–2456.
11 J. H. Na, H. Koo, S. Lee, K. H. Min, K. Park, H. Yoo, S. H. Lee, J. H. Park, I. C. Kwon, S. Y. Jeong and K. Kim, *Biomaterials*, 2011, **32**, 5252–5261.
12 H. Prichystalova, N. Almonasy, A. M. Abdel-Mohsen, R. M. Abdel-Rahman, M. M. Fouda, L. Vojtova, L. Kobera, Z. Spotz, L. Burgert and J. Jancar, *Int. J. Biol. Macromol.*, 2014, **65**, 234–240.
13 F. Lebouc, I. Dez, J. Desbrières, L. Picton and P.-J. Madec, *Polymer*, 2005, **46**, 639–651.
14 K. Tommeraas, M. Koping-Hoggard, K. M. Varum, B. E. Christensen, P. Artursson and O. Smidsrod, *Carbohydr. Res.*, 2002, **337**, 2455–2462.
15 M. Morimoto, M. Nakao, N. Ishibashi, Y. Shigemasa, S. Ifuku and H. Saimoto, *Carbohydr. Polym.*, 2011, **84**, 727–731.

16 S. P. McManus, A. Kozlowski and P. D. Youso, *Monoconjugated Chitosans as Delivery Agents for Small Interfering Nucleic Acids, US Pat.*, US 8916693, 2010.
17 S. K. Tripathi, R. Goyal, M. P. Kashyap, A. B. Pant, W. Haq, P. Kumar and K. C. Gupta, *Biomaterials*, 2012, **33**, 4204–4219.
18 B. E. Benediktsdottir, K. K. Sorensen, M. B. Thygesen, K. J. Jensen, T. Gudjonsson, O. Baldursson and M. Masson, *Carbohydr. Polym.*, 2012, **90**, 1273–1280.
19 J. M. Los, L. B. Simpson and K. Wiesner, *J. Am. Chem. Soc.*, 1956, **78**, 1564–1568.
20 K. Tømmeraas, K. M. Vårum, B. E. Christensen and O. Smidsrød, *Carbohydr. Res.*, 2001, **333**, 137–144.
21 E. P. Azevedo, S. V. Santhana Mariappan and V. Kumar, *Carbohydr. Polym.*, 2012, **87**, 1925–1932.
22 G. G. Allan and M. Peyron, *Carbohydr. Res.*, 1995, **277**, 257–272.
23 D. Filion, M. Lavertu and M. D. Buschmann, *Biomacromolecules*, 2007, **8**, 3224–3234.
24 R. Novoa-Carballal and A. H. E. Muller, *Chem. Commun.*, 2012, **48**, 3781–3783.
25 R. Novoa-Carballal, C. Silva, S. Moller, M. Schnabelrauch, R. L. Reis and I. Pashkuleva, *J. Mater. Chem. B*, 2014, **2**, 4177–4184.
26 T. O. Eloranta, A. R. Khomutov, R. M. Khomutov and T. Hyvonen, *J. Biochem.*, 1990, **108**, 593–598.
27 J. Kalia and R. T. Raines, *Angew. Chem., Int. Ed.*, 2008, **47**, 7523–7526.
28 T. S. Zatsepin, D. A. Stetsenko, A. A. Arzumanov, E. A. Romanova, M. J. Gait and T. S. Oretskaya, *Bioconjugate Chem.*, 2002, **13**, 822–830.
29 J. Shao and J. P. Tam, *J. Am. Chem. Soc.*, 1995, **117**, 3893–3899.
30 G. E. Lienhard and W. P. Jencks, *J. Am. Chem. Soc.*, 1966, **88**, 3982–3995.
31 E. G. Sander and W. P. Jencks, *J. Am. Chem. Soc.*, 1968, **90**, 6154–6162.
32 M. P. Schubert, *J. Biol. Chem.*, 1936, **114**, 341–350.
33 R. E. Barnett and W. P. Jencks, *J. Am. Chem. Soc.*, 1967, **89**, 5963–5964.
34 R. Caraballo, H. Dong, J. P. Ribeiro, J. Jiménez-Barbero and O. Ramström, *Angew. Chem.*, 2010, **122**, 599–603.
35 E. Campaigne, in *Organic Sulfur Compounds*, ed. N. Kharasch, Pergamon, Oxford, 1961, pp. 134–145.
36 T. W. G. Peter and G. M. Wuts, in *Protective groups in organic synthesis*, ed. Wiley, 2006, ch. 4, pp. 477–500.
37 R. Lumry, E. L. Smith and R. R. Glantz, *J. Am. Chem. Soc.*, 1951, **73**, 4330–4340.
38 S. Claustre, F. Bringaud, L. Azéma, R. Baron, J. Périé and M. Willson, *Carbohydr. Res.*, 1999, **315**, 339–344.
39 M. Erlandsson and M. Hällbrink, *Int. J. Pept. Res. Ther.*, 2005, **11**, 261–265.
40 M. Lavertu, Z. Xia, A. N. Serreqi, M. Berrada, A. Rodrigues, D. Wang, M. D. Buschmann and A. Gupta, *J. Pharm. Biomed. Anal.*, 2003, **32**, 1149–1158.
41 M. Lavertu, V. Darras and M. D. Buschmann, *Carbohydr. Polym.*, 2012, **87**, 1192–1198.
42 S. Nguyen, F. M. Winnik and M. D. Buschmann, *Carbohydr. Polym.*, 2009, **75**, 528–533.
43 D. Banfi and L. Patiny, *Chimia*, 2008, **62**, 280–281.
44 M. Lavertu, S. Méthot, N. Tran-Khanh and M. D. Buschmann, *Biomaterials*, 2006, **27**, 4815–4824.
45 Y. Niebel, M. D. Buschmann, M. Lavertu and G. De Crescenzo, *Biomacromolecules*, 2014, **15**, 940–947.
46 R. Bell, *Adv. Phys. Org. Chem.*, 1966, **4**, 1–29.
47 L. Heux, J. Brugnerotto, J. Desbrières, M. F. Versali and M. Rinaudo, *Biomacromolecules*, 2000, **1**, 746–751.
48 J. L. Axson, K. Takahashi, D. O. De Haan and V. Vaida, *Proc. Natl. Acad. Sci. U. S. A.*, 2010, **107**, 6687–6692.
49 H. Saito, R. Tabeta and K. Ogawa, *Macromolecules*, 1987, **20**, 2424–2430.
50 E. M. Schulman, O. D. Bonner, D. R. Schulman and F. M. Laskovics, *J. Am. Chem. Soc.*, 1976, **98**, 3793–3799.
51 D. P. N. Satchell and R. S. Satchell, *Chem. Soc. Rev.*, 1990, **19**, 55–81.
52 L. Fournier, G. Lamaty, A. Natat and J. P. Roque, *Tetrahedron*, 1975, **31**, 1025–1029.
53 T. D. Claridge, *High-resolution NMR techniques in organic chemistry*, Newnes, 2008.
54 D. Pinto, C. M. Santos and A. M. Silva, *Recent Research Developments in Heterocyclic Chemistry*, Pinho e Melo, Research Signpost, Kerala, India, 2007.
55 A. Bax, K. A. Farley and G. S. Walker, *J. Magn. Reson., Ser. A*, 1996, **119**, 134–138.
56 J. Furrer, *Chem. Commun.*, 2010, **46**, 3396–3398.
57 A. V. Kabanov and V. A. Kabanov, *Bioconjugate Chem.*, 1995, **6**, 7–20.
58 I. K. Voets, A. de Keizer and M. A. Cohen Stuart, *Adv. Colloid Interface Sci.*, 2009, **147–148**, 300–318.
59 D. V. Pergushov, A. H. E. Muller and F. H. Schacher, *Chem. Soc. Rev.*, 2012, **41**, 6888–6901.